

Topology Optimization of a Lower Barrel in Nose Landing Gear

Anup V Patil¹, Dr. R Chandra Kumar², Rajesh Patel³

¹PG Student, Department of Mechanical Engineering, RV College of Engineering®, Bengaluru

²Assitant Professor, Department of Mechanical Engineering, RV College of Engineering®, Karnataka, India

³Engineer-II, Materials and Process Engineering, Textron India Pvt.Ltd.

Abstract – The main objective of the current work is to optimize the design of lower barrel of nose landing gear by considering weight as a predominant parameter. The topology optimization is performed at three stages: (1) CAD modelling and pre-optimization analysis of lower barrel, (2) Topology optimization of lower barrel with the objective Maximize the stiffness and (3) Post-optimization of the lower barrel. The pre-optimization of the lower barrel yielded good results, where the structural parameters such as equivalent stress (von-Mises) and shear stress which were quantified to 45.243 MPa and 7.45 MPa respectively. Further the optimization runs ensured that the mass of the lower barrel, which was initially 14.507 kg were subsequently reduced to the optimization runs were carried out the mass was reduced to 13.151, 12.785, 12.703, 12.654 and 12.579 kg in successive runs with no change in the quantifications of structural properties in comparison with pre-optimization results. Considering the optimization runs and assembly constraints, the final optimized model weighed 10.378 kg, whereas the structural properties such as equivalent stress and shear stress had deviation of 1.88 and 3.06 % respectively from the initial results. The outcome of the research work is that the weight of the lower barrel was reduced and the design was optimized.

Key Words: Landing Gear, Design Optimization, Topology Optimization, Lower Barrel, Design and Non-Design space.

1.INTRODUCTION

As the global interactions continue to expand, there will be a subsequent raise in demand for aviation as the prime mode of transportation. The International Air Transport Association (IATA) has come up with the figures that the air travelers will be increased from 3.8 billion as of 2016 to 7.6 billion by the end of 2035 [1]. The forecast for passenger growth confirms that the biggest demand will be the Asia-Pacific region. China will replace US as the world's largest aviation market around 2024, while India displaces UK from the third position as shown in the Figure 1.

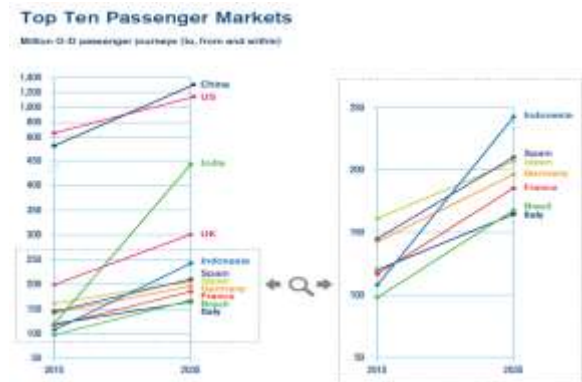


Fig -1: Growth of Aviation Market [1]

Although the payload contributes the least to the MTOW in most cases, approximately 20%, it still represents an important area for the aerospace industry to optimize [3]. The remaining 50% to 60% of the MTOW is from the OEW of an aircraft and is the main area of focus for introducing weight savings. Since an aircraft is comprised of many different components and subsystems, there is a vast amount of research going into various aspects and parts of aircraft design [2,3]. Though there has been a significant advancement in the aerospace field, there are still good number of components where weight reduction of the same proves to be difficult due to various complexities tied with the system. One such challenge to optimize arises in the landing gear system of an aircraft

2. LANDING GEAR

Landing gear is an undercarriage for aircrafts used to absorb the impact of the landing operation and also to perform ground operations starting from taxiing to halting or vice versa. Both dynamic and static loads act on the landing gear. But dynamic and static analysis are conducted sequentially or independently due to computational restrictions even though dynamic and static loads are dependent to each other [4]. Landing gears include tires, brakes and oleo. For the passengers and engineers, the landing gear is nothing but a set of wheels, but there are a lot of demanding functions which is described in [5].

2.1 Landing Gear Components

In order to gain a better understanding of the landing gear design process, the nomenclature typically used to identify

materials, structural layouts, component layout and fastener layout design. Topology optimization by itself has a variety of methods, which are homogenization-based method, evolutionary structural optimization, density-based approach, bubble method, topological derivative, phase field method and level set method.

5. COMPUTATIONAL MODEL AND PRE-OPTIMIZATION ANALYSIS

A CAD model of lower barrel was modelled using CATIA-V5 as shown in the Figure 3 and a pre-optimization analysis was performed using ANSYS 18.1, where SOLID 187 3D tetrahedron element was used for meshing as shown in the Figure 4, with element size of 1.5 mm. The quality of the mesh is fine. The total number of nodes used to create the mesh is 1320486 and the number of elements quantifying up-to 413121. The material of the lower barrel is AISI 4130 Steel.

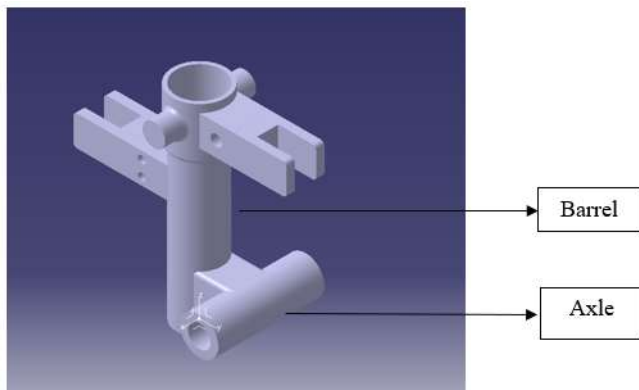


Fig -3: CAD Model of Lower Barrel

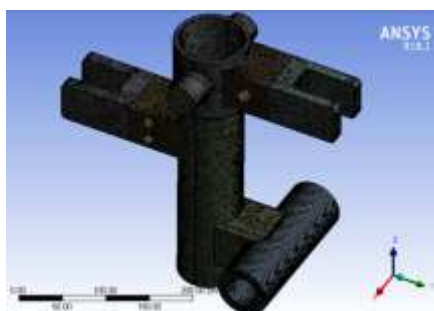


Fig -4: Meshed Model of Lower Barrel

There are nearly 300-400 load cases acting on the landing gear assembly calculated using the MBD analysis concept, lower barrel being the critical component where the worst loading scenario acts when an aircraft land. Considering the weight of the aircraft to be approximately 8000 kg, the maximum landing weight is approximately 13000 kg which creates a reaction force of about 127.489 kN on the lower barrel of the MLG. By the time NLG touches the ground the load acting on the lower barrel will be reduced and it is quantified to 30 kN which is the spin-up case.

The spin-up impact case is considered as the static load for analyzing and optimizing the lower barrel of NLG to confirm the structural stability. The static load of 30 kN is acting on the inner surface of the Axle in the positive Z-direction. The ends of the axle and top surface of the lower barrel are fixed as shown in the Figure 5.

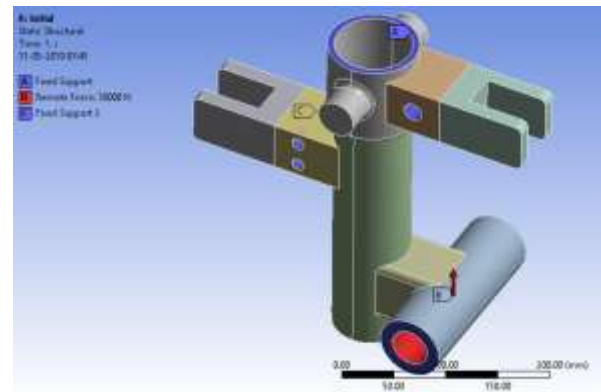


Fig -5: Boundary Conditions for Pre-optimization Analysis

The pre-optimization analysis yielded good results with structural properties such as equivalent (von-Mises) stress and shear stress being quantified to 45.243 MPa and 7.45 MPa as shown in the Figures 6 and 7.

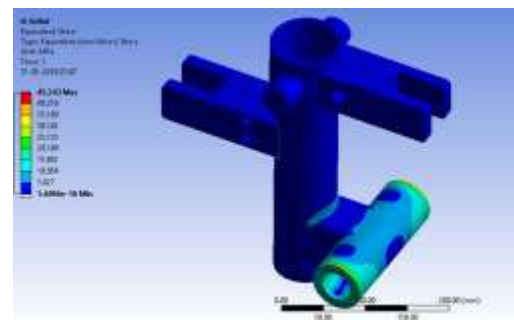


Fig -6: Equivalent (von-Mises) stress of Lower Barrel

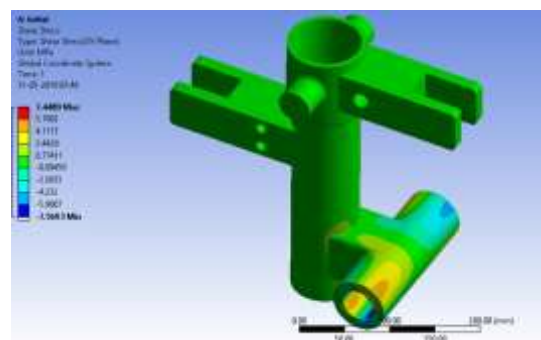


Fig -7: Shear Stress of Lower Barrel

6 Topology Optimization of Lower Barrel and Post-Optimization Analysis

The next stage of the work involves the topology optimization of lower barrel. By considering the boundary conditions called out in the section 5, topology optimization is performed in iterations using Altair Inspire software 2.1 and at each iteration the design is revised based on the inputs obtained by optimization. The design at each iteration is subjected to analysis to check for the structural stability which is being compared with the pre-optimization results.

6.1 Design and Non-Design Space Designation

The first step of the topology optimization is to define the design and non-design space for the lower barrel. Design spaces are such area which is considered for the optimization, these are the areas which are neither subjected to loads nor any kind of supports or assembly constraints. Non-design spaces are such areas which are not supposed to be altered as these regions are either subjected to load cases or these are the various locations where another component comes in contact as an assembly constraint.

The lower barrel was segmented into design and non-design spaces as shown in the Figure 8. Design space is represented by brown color and the non-design space with greyish color. The axle part is designated as non-design space as the entire inner surface is subjected to load case. Torque links gets attached to the holes represented in the lower barrel, by the definition of non-design space it is evident that connecting surfaces must be designated as non-design space.

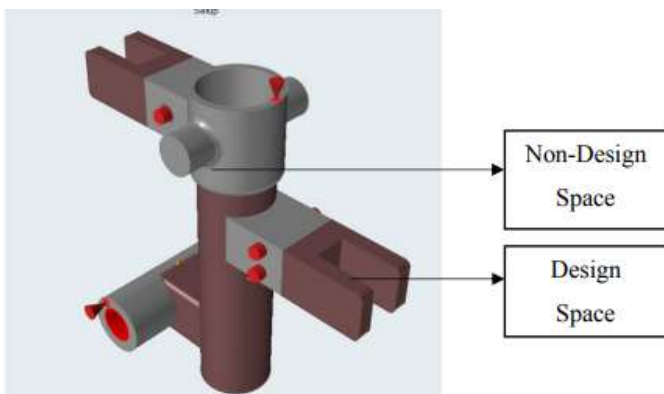


Fig -8: Designation of Design Space of Lower Barrel

6.2 Optimization Run

In Altair Inspire, after the designation of design space and applying the boundary conditions, load cases on the lower barrel, optimization run option is selected and the following inputs are provided as shown in the Figure 9.

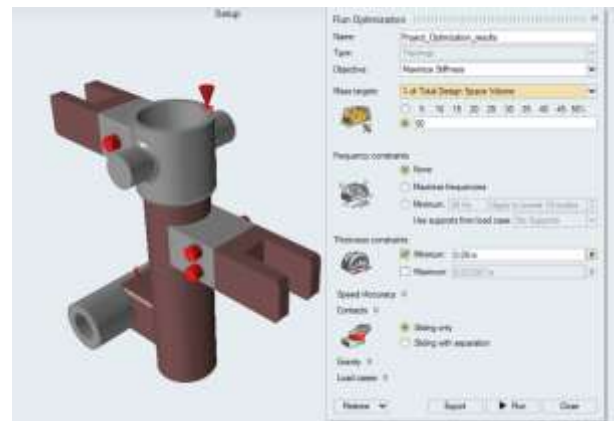


Fig -9: Set-up for Optimization

6.2.1 Maximize the Stiffness

The objective chosen to run the optimization is “Maximize the Stiffness”. The lower barrel component of the NLG being one of the crucial components and the worst loading case is acting on it, the component must be designed stiffer. Here in the objective maximize stiffness, it is needed to specify the mass targets (the amount of material needs to be retained) of the total design space in terms of percentage as shown in the Figure 10, while other input parameters being same as minimize the mass.

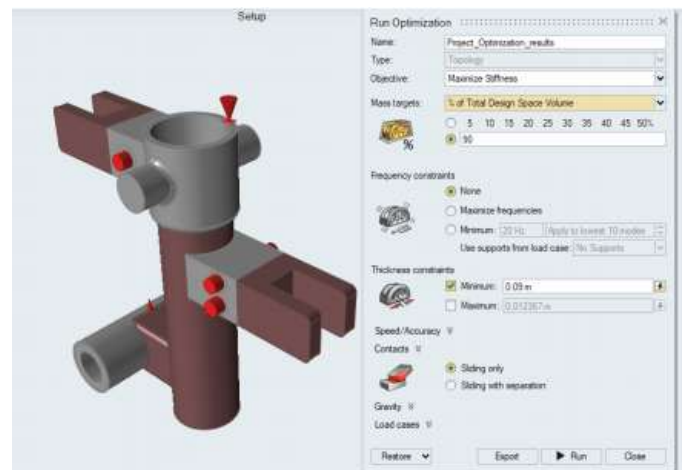


Fig -10: Maximize the Stiffness- 90 % Volume Retention

6.3 Interpretation of the Optimization Results of Lower Barrel

Simultaneously as the optimization is performed and at the end of each iteration the optimized model from Altair Inspire is imported to CATIA-V5 to refine the contours of the lower barrel as the design obtained from Altair Inspire is in coarse form and cannot be manufactured easily. With this context the optimized models are redesigned using CATIA-V5 and for representation purpose the models at 90 %, 75 % and 60 % volume retention are considered which is explained in further sections. These models after being redesigned, are

subjected to various boundary conditions and load cases as that of the initial case as explained in chapter 4 to ensure that the design is safe as the initial case.

6.3.1 Interpretation for 90 % Volume Retention

The first run of optimization was done by retaining 90 % of the total volume of design space which resulted in reducing the mass of the lower barrel from 14.507 to 13.151 kg by removing the un-wanted mass from the component, which was not significant as it was not subjected to any loading conditions. The optimized model as shown in the Figure 11 was imported to CATIA-V5 and it was re-designed as shown in the Figure 11.

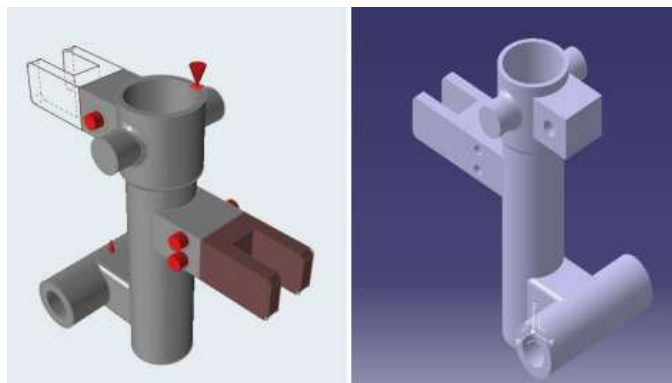


Fig -11: (a) Optimized Model and (b) Re-designed Model at 90 % Volume Retention

The re-designed model as shown in the Figure 5.15(b) was then analyzed using ANSYS 18.1 by applying the boundary conditions and loading cases as the initial case, the optimized model at this stage was meshed using SOLID 187, 3D-tetrahedron element, as shown in the Figure 5.16, with its size being 1.5mm. The total number of elements is 390918 and total number of nodes 1282362. The mesh properties are described in Table 1.

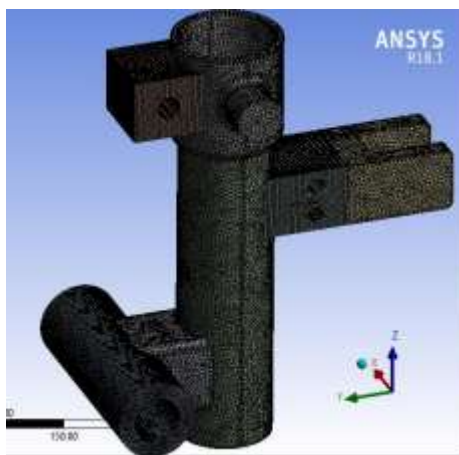


Fig -12: Meshed Model of Lower Barrel at 90 % Volume Retention

Various parameters such as equivalent stress(von-Mises) distribution, total deformation, shear stress and major principal stress are evaluated based on the ANSYS results and are quantified to 45.243 MPa, 7.45 MPa as shown in the Figures 13 and 14 respectively.

Table -1: Mesh Properties of Lower Barrel at 90 % Volume Retention

Object Name	Mesh
State	Solved
Display	
Display Style	Body Color
Defaults	
Physics Preference	Mechanical
Relevance	0
Element Order	Program Controlled
Sizing	
Size Function	Adaptive
Relevance Center	Fine
Element Size	1.5mm
Initial Size Seed	Assembly
Transition	Fast
Span Angle Center	Coarse
Automatic Mesh Based Defeaturing	On
Defeature Size	Default
Minimum Edge Length	6.64970 mm
Statistics	
Nodes	1282362
Elements	390918

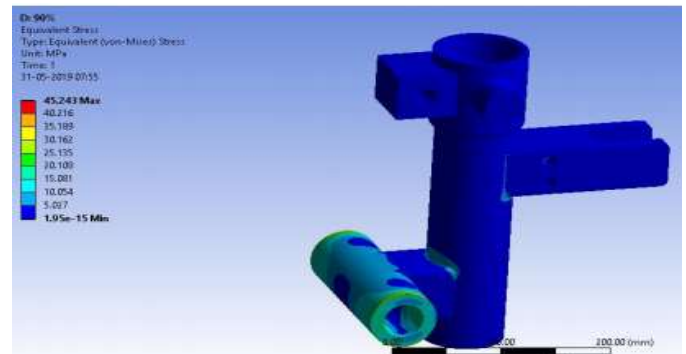


Fig -13: Equivalent Stress (von-Mises) distribution of Optimized Model at 90 % Volume Retention

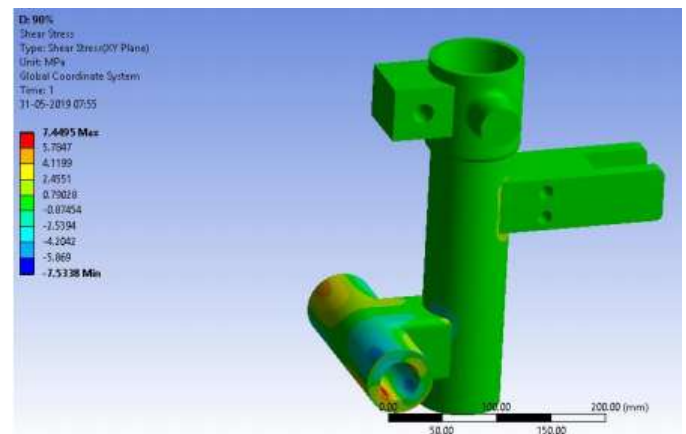


Fig -14: Shear Stress of Optimized Model at 90 % Volume Retention

Similarly, the optimization was carried at 75 and 60% volume retention, there was mass reduction of 11.88 and 13.72 % from the initial mass of lower barrel.

7. FINAL DESIGN OF LOWER BARREL

From the interpretations made in the previous chapter, it was evident further optimization based on the boundary conditions and loading cases were not required as the results of static analysis remained same through-out the optimization iterations. But it is very important to consider the assembly constraints for optimizing the lower barrel.

7.1 Final Optimized Model of Lower Barrel

Once the final optimized model was obtained at 60 % volume retention, the optimization runs were stopped, and the assembly constraints were considered for further optimization. Various components like Torque links are connected to the top surface of the lower barrel and the wheels are connected to the axle part. Considering these aspects and the smooth movement of these components in-line with the lower barrel during landing of an aircraft the final optimized model is re-designed as shown in the Figure 15.



Fig -15: Final Detailed and Optimized Model of Lower Barrel

7.2 Analysis Set-up for Final Optimized Model of Lower Barrel

The optimized model is then imported to ANSYS 18.1 to perform the static analysis to evaluate the structural behavior of the same. The boundary conditions and the loading cases remains the same as the initial model. The ends of the axle and the top surface of the barrel are fixed with load being applied on to the inner surface of the axle as shown in the Figure 16.

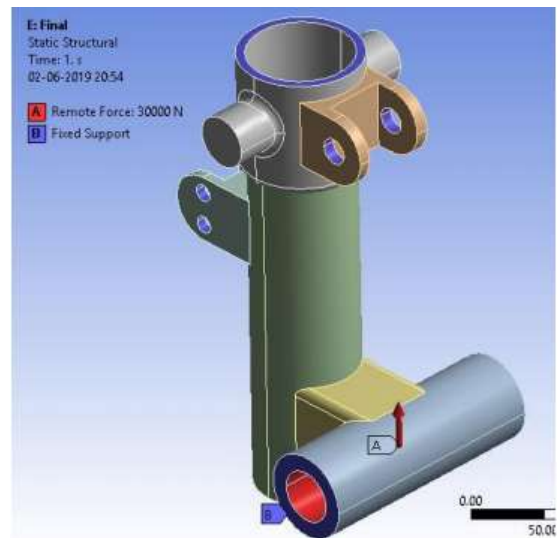


Fig -16: Boundary Conditions for Final Optimized Model of Lower Barrel

The final optimized model of lower barrel is meshed similar to the initial model of lower barrel with SOLID 187, 3D tetrahedron element with element size being 1.5mm and the quality of the mesh is fine. A total of 285262 elements were created with 822268 nodes as shown in the Figure 17.

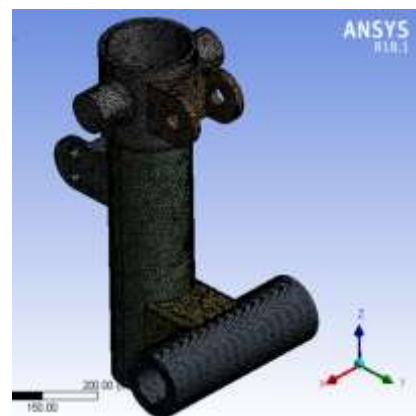


Fig -17 Meshed Model of Final Optimized Lower Barrel

The structural parameters such as equivalent (von-Mises) stress and shear stress is evaluated as shown in the Figure 18 and 19, which are quantified to 46.11 MPa and 7.23MPa.

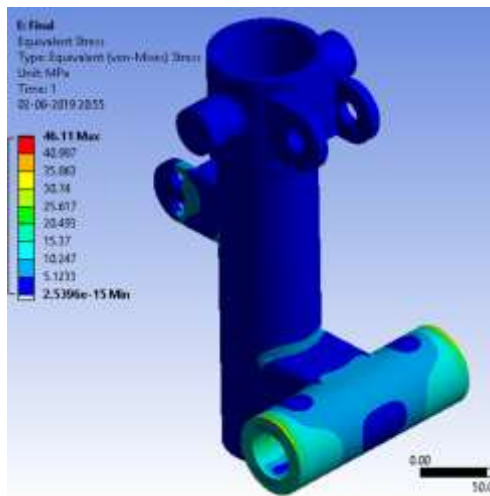


Fig -18: Equivalent Stress (von-Mises) distribution of Final Optimized Model

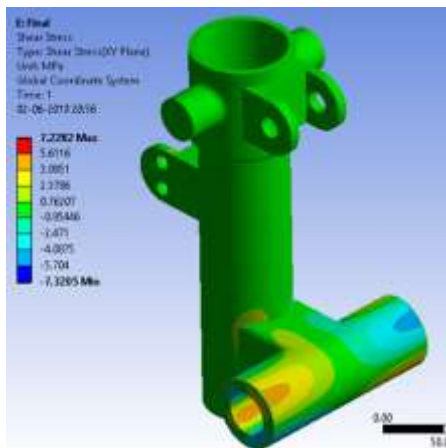


Fig -19: Shear Stress of Final Optimized Model

7.3 Comparison of Optimization Results

As the analysis of the final optimized model was performed it is very important to compare the results of topology optimization and the various structural parameters for each iteration and compute the % error occurred for each of the parameter. The results are summarized in Table 2.

Table -2: Comparison of Optimization Results of Lower Barrel of NLG

	Initial Design	Optimised Design (% of Volume Retention)			Final Design	% Error between Initial and Final Design
		90	75	60		
Mass of Lower Barrel, kg	14.507	13.151	12.785	12.579	10.378	-
Reduction of Mass, %	-	9.35	11.88	13.72	28.46	-
Equivalent Stress, MPa	45.243	45.243	45.243	45.243	46.11	1.88
Shear Stress, MPa	7.45	7.45	7.45	7.45	7.23	3.04

8. CONCLUSION

The Lower Barrel, component of the NLG was created, and the material assigned was AISI 4130 Steel. A Pre-optimization analysis was carried out which yielded the results for various static parameters such as equivalent stress (von-Mises) and shear stress which were quantified to 45.243 MPa, and 7.45 MPa respectively. Initially the mass of the lower barrel was 14.507 kg, as the optimization runs were carried out the mass was reduced to 13.151, 12.785, 12.703, 12.654 and 12.579 kg in successive runs with the analysis results of static parameters such as equivalent stress (von-Mises) and shear stress remained same as the initial run. Finally, the model was further optimized considering the optimization results and assembly constraints where the mass of the lower barrel was reduced up-to 28.46%, which was easy to manufacture. The final optimized and detailed lower barrel weighed up-to 10.378 kg which is a considerable value of topology optimization. To conform the structural stability post-optimization analysis was carried out where the equivalent stress, total deformation and shear stress had deviation of 1.88 and 3.04 % respectively from the initial results.

REFERENCES

- [1] International Air Transport Association, "IATA Forecasts Passenger Demand to Double Over 20 Years," IATA Press Release No. 59, no. October, 2016, pp. 18–22.
- [2] Fordham R.C, "Airport Planning in the Context of the Third London Airport," Econ. J., vol. 80, no. 3183, pp. 307–322, 1970.
- [3] L. News, "Updating the A380: the prospect of a neo version and what's involved," pp. 1–5, 2014.
- [4] Hitch H.P.Y, "Aircraft Ground Dynamics," Veh. Syst. Dyn., vol. 10, no. 4–5, pp. 319–332, 1981.
- [5] Krüger W.R, Besselink I.J, Cowling. D, Doan D.B, Kortüm. W, and Krabacher. W, "Aircraft Landing Gear Dynamics: Simulation and Control," Veh. Syst. Dyn., vol. 28, no. 2–3, pp. 119–158, 1997.
- [6] Federal Aviation Authority, "Chapter 13 - Aircraft Landing Gear Systems," Aviat. Maint. Tech. Handb. - Airframe, pp. 20–22, 2014.
- [7] Pritchard. J, "Overview of Landing Gear Dynamics," J. Aircr., vol. 38, no. 1, pp. 130–137, 2001.
- [8] AGARD Report, The Design, Qualification and Maintenance of Vibration-Free Landing Gear (R-800), no. October. 1995.
- [9] Denti. E and Fanteria. D, "Models of Wheel Contact Dynamics: An Analytical Study on the In-Plane Transient

Responses of a Brush Model," Veh. Syst. Dyn., vol. 34, no. December 2012, pp. 37-41, 2010.

[10] Tadeusz. N, Jerzy. M, and Adam. B, "Numerical Analysis of a Front Support Landing Gear Dynamics," pp. 3-10, 2006.

[11] Besselink I.J.M, Shimmy of Aircraft Main Landing Gears. Delft, Netherlands: Delft University of Technology, 2000.

[12] Gowda A.C, "Trends in Mechanical Engineering & Technology Linear Static and Fatigue Analysis of Nose Landing Gear for Trainer Aircraft," vol. 4, no. 2, pp. 1-10, 2014.

[13] Nguyen T, Schonning A, Eason P, and Nicholson D, "Methods for Analyzing Nose Gear During Landing Using Structural Finite Element Analysis," J. Aircr., vol. 49, no. 1, pp. 275-280, 2012.

[14] Luenberger D.G and Ye. Y, Linear and Nonlinear Programming, vol. 228, 2016.

[15] Sigmund O, "A 99 line topology optimization code written in MATLAB," Struct. Multidiscip. Optim., vol. 21, no. 2, pp. 120-127, 2001.

[16] Svanberg K, "MMA and GCMMA - two methods for nonlinear optimization," Technical Report, 2007.